

## Article

# Untargeted Metabolomics Combined with Metabolic Flux Analysis Reveals the Mechanism of Sodium Citrate for High S-Adenosyl-Methionine Production by *Pichia pastoris*

Wentao Xu <sup>†</sup>, Feng Xu <sup>†</sup> , Weijing Song, Le Dong, Jiangchao Qian and Mingzhi Huang <sup>\*</sup>

State Key Laboratory of Bioreactor Engineering, East China University of Science and Technology, No. 130 Meilong Road, Shanghai 200237, China

<sup>\*</sup> Correspondence: huangmz@ecust.edu.cn<sup>†</sup> These authors contributed equally to this work.

**Abstract:** S-adenosyl-methionine (SAM) is crucial for organisms to maintain some physiological functions. However, the inconsistency between high L-methionine feeding rate and yield during SAM production at an industrial scale and its metabolic mechanism have not been elucidated. Here, the cellular metabolic mechanism of feeding sodium citrate to the *Pichia pastoris* (*P. pastoris*) G12' / AOX-acs2 strain to enhance SAM production was investigated using untargeted metabolomics and metabolic flux analysis. The results indicated that the addition of sodium citrate has a facilitative effect on SAM production. In addition, 25 metabolites, such as citrate, cis-aconitate, and L-glutamine, were significantly up-regulated, and 16 metabolites, such as glutathione, were significantly down-regulated. Furthermore, these significantly differential metabolites were mainly distributed in 13 metabolic pathways, such as the tricarboxylic acid (TCA) cycle. In addition, the metabolic fluxes of the glycolysis pathway, pentose phosphate pathway, TCA cycle, and glyoxylate pathway were increased by 20.45–29.32%, respectively, under the condition of feeding sodium citrate compared with the control. Finally, it was speculated that the upregulation of dihydroxyacetone level might increase the activity of alcohol oxidase AOX1 to promote methanol metabolism by combining metabolomics and fluxomics. Meanwhile, acetyl coenzyme A might enhance the activity of citrate synthase through allosteric activation to promote the flux of the TCA cycle and increase the level of intracellular oxidative phosphorylation, thus contributing to SAM production. These new insights into the L-methionine utilization for SAM biosynthesis by systematic biology in *P. pastoris* provides a novel vision for increasing its industrial production.

**Keywords:** *Pichia pastoris*; S-adenosyl-methionine; sodium citrate; untargeted metabolomics; metabolic flux analysis



**Citation:** Xu, W.; Xu, F.; Song, W.; Dong, L.; Qian, J.; Huang, M. Untargeted Metabolomics Combined with Metabolic Flux Analysis Reveals the Mechanism of Sodium Citrate for High S-Adenosyl-Methionine Production by *Pichia pastoris*. *Fermentation* **2022**, *8*, 681. <https://doi.org/10.3390/fermentation8120681>

Academic Editor: Hao Li

Received: 11 October 2022

Accepted: 24 November 2022

Published: 27 November 2022

**Publisher's Note:** MDPI stays neutral with regard to jurisdictional claims in published maps and institutional affiliations.



**Copyright:** © 2022 by the authors. Licensee MDPI, Basel, Switzerland. This article is an open access article distributed under the terms and conditions of the Creative Commons Attribution (CC BY) license (<https://creativecommons.org/licenses/by/4.0/>).

## 1. Introduction

S-adenosyl-methionine (SAM) is an endogenous intracellular amino acid metabolite and enzyme co-substrate involved in various vital biochemical pathways [1–3]. A positively charged S atom adjacent to the SAM electron C atom yields SAM the ability to participate in three crucial biochemical pathways, including transmethylation, transsulfuration, and polyamine synthesis [4,5]. In addition, as an essential methyl donor in living organisms, SAM is also involved in many reactions in living organisms, including the synthesis of various nucleic acids, proteins, phospholipids, and vitamins [6]. *Pichia pastoris* (*P. pastoris*) is commonly applied as an expression host for SAM synthesis [3,6]. Moreover, *P. pastoris* is widely used in the industrial production of various proteins compared with *Escherichia coli* (*E. coli*) and *Saccharomyces cerevisiae* (*S. cerevisiae*) owing to its high-density growth, stable recombinant gene expression, and the ability to grow with methanol as a single carbon source [7].

As direct precursors of SAM biosynthesis, both L-methionine and ATP concentrations during fermentation will directly affect the final SAM yield during *P. pastoris* fermentation. Previous studies have recognized that SAM production can be further enhanced by boosting the intracellular ATP level [8–10]. Hu et al. modified the substrate supplementation in the induction phase of *P. pastoris* by upgrading the traditional methanol supplementation to alternating glycerol-methanol supplementation. The results showed a significant increase in intracellular ATP and SAM concentrations [11]. The industrial production of SAM is commonly based on the over-supplementation of the precursor L-methionine to increase the yield [6,12]. However, L-methionine is not only present in the medium as a synthetic precursor of SAM, but also as a source of carbon and nitrogen necessary for microbial growth under some conditions.

Metabolomics and metabolic fluxomics are often employed to describe alterations in cellular metabolism, as well as to explain the phenotype of organisms [13,14]. It is applicable to many fields, including plants, animals, synthetic biology, and medicine [15]. The qualitative and quantitative analysis of small molecule compounds allows the identification of modifications in metabolic pathways. Recently, metabolomics and metabolic fluxes have been applied further to analyze the intracellular metabolic network of *P. pastoris* and quantify intracellular metabolites to guide production for yield improvement [16–18]. For instance, Liu et al. integrated quantitative metabolomics and isotopic non-stationary metabolic flux analysis to provide insight into the mechanism underlying the effect of glutamate addition on the further enhancement of  $\beta$ -galactosidase production in high-yielding strains [16]. Nie et al. investigated the effect of different heterologous protein expression levels comprehensively on the physiological metabolism under the culture conditions with glucose as the sole carbon source by  $^{13}\text{C}$  metabolic flux analysis [17]. Jorda et al. explored the metabolism of *P. pastoris* using  $^{13}\text{C}$  quantitative metabolomics and non-stationary  $^{13}\text{C}$  metabolic flux methods [18]. However, overexpression of recombinant proteins could trigger metabolic burdens in *P. pastoris*, such as increased demand for energy (ATP) as well as reducing cofactor (NADPH), affecting not only protein expression but also cell growth [19,20]. Therefore, it is of great significance to learn the variations of intracellular metabolite content and intracellular energy as well as the reducing power metabolism of *P. pastoris* when expressing SAM. Previous studies have shown that the optimal L-methionine feeding rate during *P. pastoris* fermentation in a 5 L bioreactor was 0.2 g/L/h [11,12]. Meanwhile, the optimal rate of L-methionine supplementation in a 15 L reactor was 0.4 g/L/h. However, it was found that the yield of SAM decreased significantly when the L-methionine feeding rate was further increased [6,10]. The solutions identified for this status and the analysis of the cellular metabolic mechanisms have rarely been reported [9].

In this study, sodium citrate was used as an effective substrate to enhance SAM production when feeding with L-methionine at a rate of 0.4 g/L/h. To further explore the mechanism of sodium citrate on SAM production during *P. pastoris* fermentation, samples were analyzed by non-targeted metabolomics techniques. Subsequently, the intracellular differential metabolites that showed significant changes after the addition of sodium citrate and the metabolic pathways that were significantly enriched with the relevant differential metabolites were screened. Finally, the possible cellular mechanism of feeding sodium citrate on the SAM production of *P. pastoris* was analyzed in combination with metabolic flux analysis. The results showed that the addition of sodium citrate promoted the metabolic flux of the TCA cycle and intracellular oxidative phosphorylation level; the intracellular energy limitation caused by excessive L-methionine supplementation was thus alleviated effectively. The results of this study aim to deepen the understanding of the metabolic properties of SAM synthesis in *Pichia pastoris*, which is essential for promoting efficient SAM synthesis.

## 2. Materials and Methods

### 2.1. Strain and Cultivations

The *P. pastoris* G12' / AOX-acs2 strain was grown on YPD medium (yeast extract 1%, peptone 2%, glucose 2%) at 30 °C for 3–4 days according to the previous report [10]. Colonies of *P. pastoris* were picked on the plate and inoculated into a 250 mL shake flask, with 25 mL YPD medium at 220 rpm and 30 °C for 20 h. Then, 5 mL of primary seed culture was transferred into a 500 mL shake flask containing 50 mL of YPG medium (yeast extract 1%, peptone 2%, glycerol 2%) and incubated for 16 h at 220 rpm and 30 °C until OD<sub>600</sub> reached 15–20 for fermentation. The fed-batch cultivation of *P. pastoris* was cultured in a 5-L bioreactor and monitored by an advanced control system *Biostar* (Shanghai Guoqiang Bio-engineering Equipment Co., Ltd., Shanghai, China). Process mass spectrometer (MAX300-LG, Extrel, Pittsburgh, PA, USA) was used to determine the O<sub>2</sub> and CO<sub>2</sub> concentrations during fermentation. The pH was fixed at 5.5 and controlled by 25% NH<sub>3</sub>·H<sub>2</sub>O. A dissolved oxygen (DO) concentration of 30% saturation was maintained by adjusting the agitation and the aeration. Fermentation medium (g/L): CaSO<sub>4</sub> 0.93, K<sub>2</sub>SO<sub>4</sub> 18.2, MgSO<sub>4</sub>·7H<sub>2</sub>O 14.9 g/L, 85% H<sub>3</sub>PO<sub>4</sub> 26.8 mL/L, KOH 4.13 g/L, glycerol 40 g/L, and 12 mL/L PTM1 were added. The components of PTM1 were described by Baumann et al. (2008). In addition, L-methionine was supplemented at a certain rate (0.2 g/L/h and 0.4 g/L/h) 12 h after the start of methanol induction, and the 6 g/L of sodium citrate was complemented disposablely at 24 h. Culture samples were collected in triplicate from the bioreactor at different time points throughout the fermentation process for further analysis. The fermentation experiments were performed in triplicate.

### 2.2. Analysis Methods

The biomass and methanol concentrations were determined according to the previous report [10]. High-performance liquid chromatography (HPLC) was used to analyze the concentration of SAM in the fermentation broth, which was equipped with a Thermo-BioBasic Strong Cation-exchange (SCX) column (250 mm × 4.6 mm ID, 5 μm). The mobile phases were composed of 5 mM ammonium formate (A) and 500 mM ammonium formate (B). A gradient elution procedure was applied to separate SAM, which was carried out as follows: 0–5.00 min, 100% A; 5.01–9.00 min, 90% B; 9.01–12.00 min, 100% B; 12.01–17.00 min, 100% A. The flow rate was 1 mL/min, and the injection volume was 10 μL. The detection wavelength was 254 nm. The total run time was 3.5 min. The temperature of the column chamber was maintained at 25 °C. In addition, the extracellular methanol and L-methionine were analyzed using previously described methods [10,12]. The intracellular ATP level was measured using the ATP kit purchased from Beyotime Biotechnology (Shanghai, China) as per the manufacturer's protocol. All the analyses were conducted in duplicate.

### 2.3. Sample Preparation and LC-MS/MS Analysis

The fermentation broth was frozen in liquid nitrogen immediately and ground into a fine powder with a mortar and pestle. We added 1000 μL methanol/acetonitrile/H<sub>2</sub>O (2:2:1, v/v/v) to the homogenized solution for metabolite extraction. The mixture was centrifuged for 15 min (12,000 rpm, 4 °C). The supernatant was dried in a vacuum centrifuge. The samples were re-dissolved in 100 μL acetonitrile/water (1:1, v/v) for LC-MS analysis.

An ultra-performance liquid chromatograph (1290 Infinity LC, Agilent Technologies, Santa Clara, CA, USA) combined with a quadrupole time-of-flight instrument (AB Sciex TripleTOF 6600) was applied for analysis. Samples were analyzed using a 2.1 mm × 100 mm ACQUITY UPLC BEH 1.7 μm column for HILIC separation (waters, Ireland). The mobile phases were composed of (25 mM ammonium acetate and 25 mM ammonium hydroxide in water) A and (acetonitrile) B in both ESI positive and negative modes. A gradient elution procedure was applied to separate the analytes, which was carried out as follows: 0–1.0 min, 85% B; 1.0–11.0 min, 85–65% B; 11.0–11.1 min, 65–40% B; 11.1–15.1 min, 40% B; 15.1–15.2 min, 40–85% B; 15.2–20.2 min, 85% B.

The conditions for the ESI source were set as follows: curtain gas, ion source gas 1, and gas 2 were 30, 60, and 60, respectively; source temperature was 600 °C; IonSpray Voltage Floating was  $\pm 5500$  V. The  $m/z$  range 60–1000 Da was set to acquire in MS only acquisition, and the accumulation time for TOF MS scan was set at 0.20 s/spectra. In auto MS/MS acquisition, the instrument was formed to acquire over the  $m/z$  range 25–1000 Da, and the accumulation time for product ion scan was set at 0.05 s/spectra. Information dependent acquisition with high sensitivity mode was selected to acquire the product ion scan. The parameters were set as follows: the declustering potential, 60 V (+) and  $-60$  V (–); collision energy was fixed at 35 V with  $\pm 15$  eV; candidate ions to monitor per cycle: 10; exclude isotopes within 4 Da.

#### 2.4. Metabolic Flux Analysis

Metabolic flux analysis was performed based on the principle of metabolite balance, biochemical constraints, and the assumption of the pseudo-steady state of intracellular intermediate metabolites [13,21]. Therefore, mass balance equations for each intermediate metabolite can be obtained under these conditions. In this study, a simplified model for the *P. pastoris* G12' / AOX-acs2 strain according to the genome-scale metabolic network constructed by Ye et al. was used to estimate the metabolic flux distribution under the studied conditions [22]. The model mainly comprised 29 biochemical reactions, which contained the methanol metabolic pathway, glycolysis (EMP) pathway, pentose phosphate (PP) pathway, TCA cycle, glyoxylate cycle, SAM synthesis pathway, and exchange reactions (Table S1). The consumption rates of methanol, methionine, and sodium citrate and the production rates of SAM and carbon dioxide were involved in the metabolic flux analysis. In addition, the consumption rate of oxygen was used to validate the estimation. The mass balance reactions in the model can be expressed in matrix form as  $S \cdot V = b$ , where  $S$  is a stoichiometric matrix,  $V$  is a vector of unknown fluxes, and  $b$  is a vector corresponding to the net accumulation, input, consumption, or output of metabolites. The metabolic fluxes were calculated using the COBRA toolbox and Gurobi<sup>®</sup> Optimizer version 9.1.1 as the solver, where the stoichiometric matrix inside the metabolic network is the source of constraints.

#### 2.5. Data Processing and Statistical Analysis

The freely available XCMS software was performed to handle the MS data after using ProteoWizard MSConvert. The specific parameter settings regarding the peak picking and peak grouping were as follows: prefilter = c (10, 100), peak width = c (10, 60), centWave  $m/z$  = 10 ppm; minfrac = 0.5, mzwid = 0.025, bw = 5. The annotation of isotopes and adducts were determined by the Collection of Algorithms of MEtabolite pRofile Annotation (CAMERA). The variables with beyond 50% of the non-zero measurements in at least one group were kept among the extracted ion features. The metabolites were identified by comparing MS/MS spectra based on the internal database developed with authentic standards and  $m/z$  value (<10 ppm).

The normalized data were analyzed by the R software package (ropIs), including multivariate data analysis. The robustness of the model was assessed by the 7-fold cross-validation and response permutation testing. The significantly different metabolites were screened in positive and negative ion modes between the experimental and control groups using variable importance in projection (VIP) >1 combined with  $p$  values < 0.05 as the criteria in this study. The Student's  $t$ -test and Pearson's correlation analysis were performed to determine the significance of differences between two groups of independent samples and the correlation between two variables.

### 3. Results and Discussion

#### 3.1. Comparison of Physiology under Different L-methionine Feeding Rate

Firstly, the metabolic characteristics of *P. pastoris* were investigated in a 5-L bioreactor at 0.2 g/L/h (control batch) and 0.4 g/L/h (experimental set) L-methionine supplementation

(Figure 1). The results showed an increasing trend in the dry weight at both supplementation rates during the methanol induction phase (Figure 1a). An increase of 18.38% was observed in terms of biomass at the high feeding rate (97.47 g/L) compared with the low feeding rate (82.34 g/L) at 96 h. The SAM levels in the methanol induction phase at different methionine supplementation rates are shown in Figure 1a. The amount was 5.25 g/L under the low supplementation rate condition. In comparison, there was 4.43 g/L under the high supplementation rate, and SAM concentrations witnessed a decrease of 15.51% in the experimental group. The results indicated that the fermentation performance of the strain was reduced under the condition of excess L-methionine supplementation. Briefly, the SAM yield did not increase accordingly with the addition of more precursor L-methionine. As shown in Figure 1b, the extracellular L-methionine concentration started to accumulate in the subsequent period when each predefined L-methionine rate was supplemented 10 h after methanol induction. The residual amount of L-methionine in the fermentation broth under a high feeding rate was much higher than that in the control group due to the higher L-methionine supplementation rate, but the accumulation rate of L-methionine in both groups slowed down or even stabilized at a lower level at the later stage of fermentation. With the L-methionine replenishment in the fermentation process, the intracellular ATP content of both the control and experimental groups showed a decreasing trend. Specifically, the decreasing trend was more noticeable in the experimental group, and the intracellular ATP concentration at 24 h decreased from 5.89 nmol/gDCW to 0.70 nmol/gDCW. Overall, the intracellular ATP level was significantly lower under a high feeding rate than that in the control group, which indicated that the excessive L-methionine supplementation could trigger the intracellular ATP limitation.

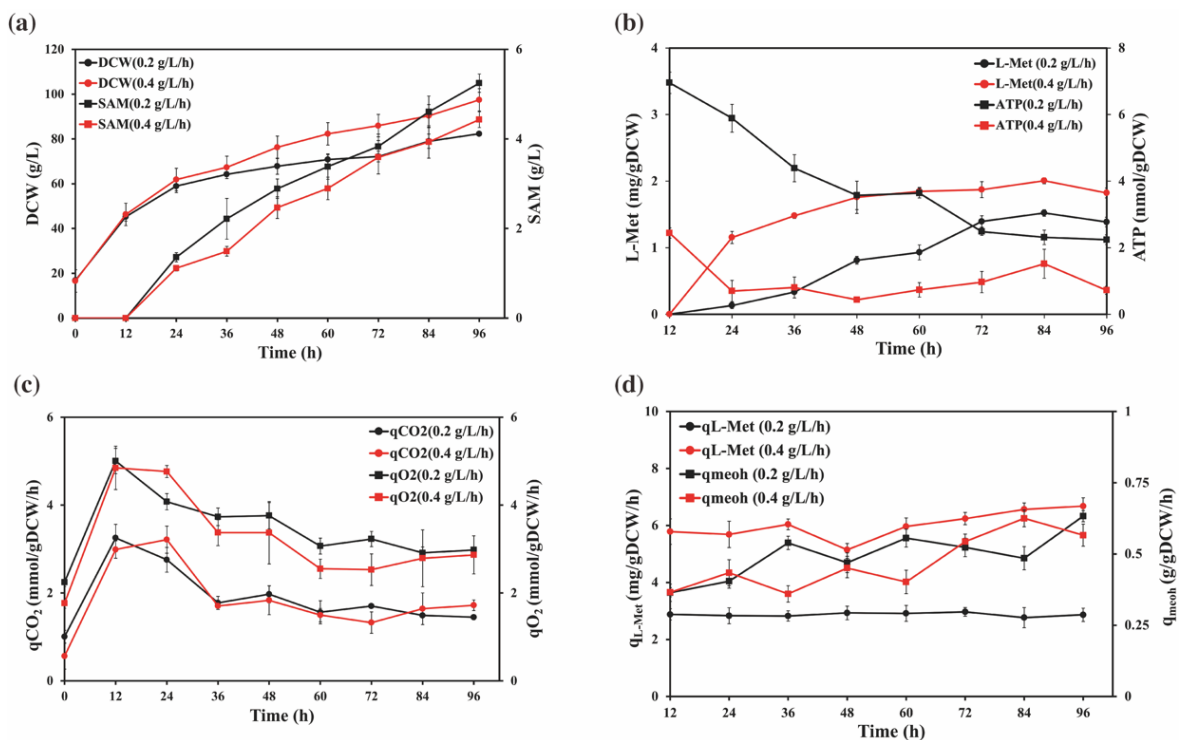


**Figure 1.** Physiological profiles of *P. pastoris* at the rate of 0.2 g/L/h and 0.4 g/L/h L-methionine supplementation in fed-batch cultivations. The parameters include (a) biomass and SAM amounts, (b) L-methionine and ATP levels, (c) specific CO<sub>2</sub> emission rate and specific O<sub>2</sub> uptake rate, and (d) specific L-methionine and methanol uptake rate. All parameters were measured based on at least triplicate measurements. The experiments were run in triplicates. The L-Met and ATP concentrations described in the figure are statistically significant.

An essential feature of cellular metabolism is the specific rate of substrate consumption and product synthesis [21]. To gain an in-depth understanding of the effects on the metabolism of *P. pastoris* at different feeding rates, the respiratory metabolic rate, specific product synthesis rate, and specific substrate consumption rate were calculated for each period. The specific carbon dioxide emission rate ( $q_{CO_2}$ ) and specific oxygen uptake rate ( $q_{O_2}$ ) in the fed-batch at 0.2 g/L/h were in a relatively stable state throughout the methanol phase (after 30 h) according to Figure 1c, indicating the feeding rate of L-methionine could provide a more stable substrate environment for the product synthesis. As seen in Figure 1d, the specific consumption rate of L-methionine in the experimental group was much higher than that in the control group. The results suggested that L-methionine might be exploited as a substrate for biomass synthesis in the later stages of fermentation. Meanwhile, the trends in terms of specific methanol consumption rates were consistent throughout the fermentation process. In addition, the results showed that the high feeding rate conditions were generally at a lower level for the specific product synthesis rate. Therefore, excessive L-methionine supplementation might lead to an energy deficit in *P. pastoris* due to the low levels of ATP reached, which affected SAM anabolism and the rest of the intracellular metabolic activities [6,10]. To this end, sodium citrate was chosen as an exogenous feeding substrate to address the situation of intracellular ATP limitation under high methionine supplementation conditions.

### 3.2. Comparison of Physiology under Sodium Citrate Supplement

To verify whether sodium citrate could play a role in alleviating intracellular energy metabolism, experiments were conducted with 6 g/L sodium citrate addition (Figure 2). The biomass in both the control (without sodium citrate) and experimental batches (with sodium citrate) showed a gradual increase (Figure 2a). The final dry weight and SAM amounts were 97.47 g/L and 4.43 g/L in the control group, and 90.68 g/L and 5.79 g/L in the experimental group, respectively. Therefore, a 34.10% decline in biomass level and a 30.55% enhancement in SAM production were observed. Furthermore, the SAM level of the experimental group was significantly higher than that of the control group in all periods. In addition, the rate of specific product generation in the experimental group was also higher than that in the control group (Figure 2b). The results indicated that the addition of sodium citrate has a facilitative effect on SAM production.

The L-methionine concentration in the control group was increasing (Figure 2c). In contrast, the L-methionine concentration in the experimental group started to fall after reaching 1.76 mg/gDCW at 48 h in the methanol induction stage. Meanwhile, the specific L-methionine consumption rate of the experimental group was also slightly higher than that of the control group, indicating that sodium citrate promoted the intracellular metabolism of L-methionine in *P. pastoris*. In addition, the intracellular ATP content decreased between the control and experimental groups (Figure 2c). However, the intracellular ATP level in the batches feeding the sodium citrate was recognizably slightly higher than that of the control group. The intracellular ATP level at 24 h increased from 0.70 nmol/gDCW to 2.42 nmol/gDCW, which indicated that the addition of sodium citrate could alleviate the intracellular energy demand, effectively improve the intracellular ATP level, and further promote SAM biosynthesis. Moreover, the specific consumption rate of the experimental group for methanol was higher than that of the control group (Figure 2d). It indicated that the rate of methanol utilization in the fermentation broth was increased after feeding sodium citrate. On the one hand, the toxic effect caused by methanol accumulation could be avoided. On the other hand, substrate utilization could be improved, and sufficient substrate supply could support product anabolism. As seen in Figure 2e, the changes of  $q_{CO_2}$  and  $q_{O_2}$  in the control and experimental groups were the same at the beginning of the induction stage. In the middle and late stages of fermentation, the experimental group was significantly higher than the control group, especially after the 6 g/L sodium citrate supplementation at 48 h. The respiratory metabolism of the experimental group

was significantly better than that of the control group. Overall, the results indicated that sodium citrate could play a vital role in improving the respiratory metabolism.

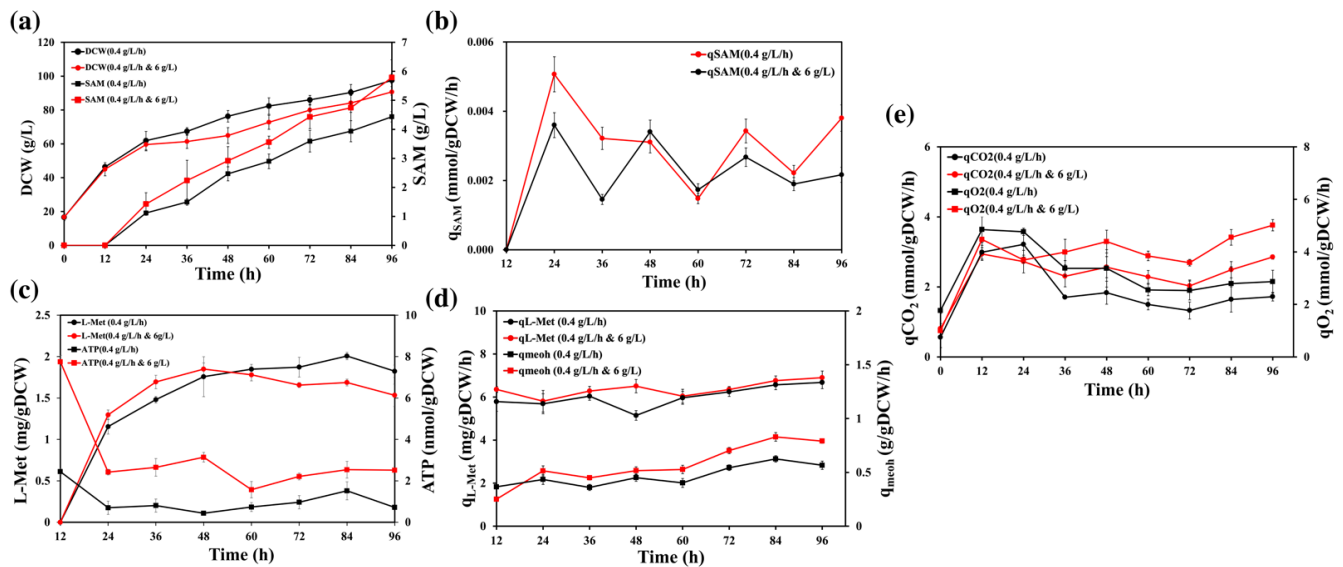


**Figure 2.** Physiological profiles of *P. pastoris* fermentation under supplementation with sodium citrate. The parameters include (a) biomass and SAM amounts, (b) specific SAM production rate, (c) L-methionine and ATP concentrations, (d) specific L-methionine and methanol uptake rate, (e) specific CO<sub>2</sub> emission rate and specific O<sub>2</sub> uptake rate. All parameters were measured based on at least triplicate measurements. The experiments were run in triplicates. The L-Met and ATP concentrations described in the figure are statistically significant.

### 3.3. Exploring the Effects of Sodium Citrate Supplementation on Cellular Metabolism through Metabolomics

To investigate the effect of sodium citrate on SAM production, the profiles of intracellular metabolites in terms of sodium citrate supplementation were further analyzed by non-targeted metabolomics. The fermentation broth from the methanol induction stage at 48 h was quenched as the control sample, and 6 g/L of sodium citrate was supplemented as the energy-assisting substrate at one time. The sample was quenched again after 1 h as the experimental group, and three biological replicates were set for each sample. The sample quality control and statistical analysis are shown in the Supplementary Materials.

#### 3.3.1. Differential Metabolite Screening and Pathway Annotation

Subsequently, 652 metabolites were identified in positive ion mode, 627 in negative ion mode, and 32 duplicate metabolites were identified in positive and negative ion mode based on the criteria. In particular, a total of 41 significantly differential metabolites were screened, among which 25 differential metabolites were up-regulated considerably, and the rest were significantly down-regulated. The detailed results of significantly differential metabolites are listed in Tables S2 and S3 under positive and negative ion modes. For instance, Di-hydroxyacetone (DHA), citric acid, cis-aconitate, L-saccharopine, and L-glutamine witnessed a significant upregulation.

The differential metabolites screened in all positive and negative ion patterns were analyzed by KEGG pathways. The results showed that these significantly differential metabolites were enriched in 56 metabolic pathways, involving 27 differential metabolites. KEGG pathway enrichment analysis was used to analyze the distribution of differential metabolites. The results showed that 13 pathways were significantly enriched (Figure 3a). Specifically, seven subsystems were related to amino acid metabolism, including amino acid biosynthesis, alanine, aspartate, and glutamate metabolism, lysine biosynthesis, lysine degradation, glutamatergic synapse,  $\gamma$ -aminobutyric acid synapse, and tyrosine

metabolism. In addition, three pathways are associated with organic acid metabolism, including glyoxalate and dicarboxylic acid metabolism, TCA cycle, and 2-oxocarboxylic acid metabolism. The remaining significantly enriched pathways were carbon fixation pathways in prokaryotes, two-component systems, and benzoate degradation, respectively.

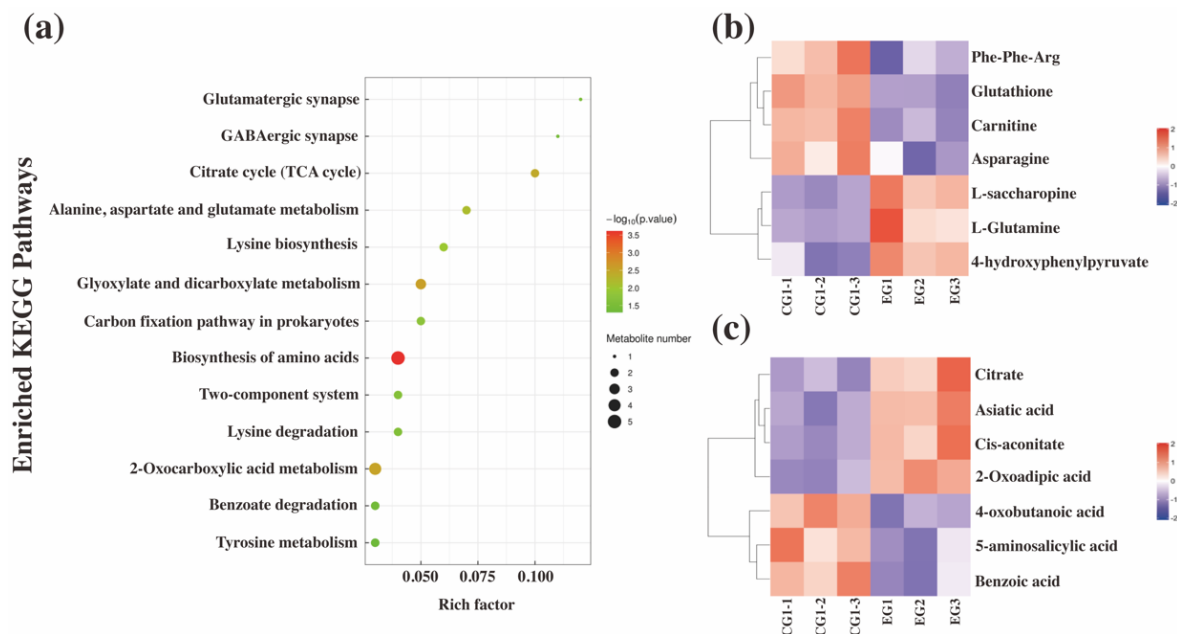


**Figure 3.** The bubble map of KEGG enrichment pathway for differential metabolites (a). Cluster analysis of significantly differential metabolite in *P. pastoris* after sodium citrate treatment. (b) Amino acid metabolism-related; (c) organic acid metabolism-related.

### 3.3.2. Clustering Analysis of Differential Metabolites Related to Amino Acid Metabolism

Amino acids are a class of organic compounds containing amino and carboxyl groups and are vital metabolites in cellular metabolism. Briefly, amino acids are precursors for the synthesis of various proteins and also form a variety of catalytically active enzymes to regulate cellular metabolism. The significantly different metabolites involved in the pathways in terms of amino acid metabolism are shown in Figure 3b. Compared with the control group, carnitine, phenylalanine, arginine, glutathione, and asparagine were significantly down-regulated. Meanwhile, L-saccharopine, L-glutamine, and 4-hydroxyphenyl pyruvate were significantly up-regulated in the experimental group.

Specifically, the  $\alpha$ -ketoglutarate (AKG) and the ATP produced via the oxidative phosphorylation pathway provided sufficient precursors for glutamine synthesis after feeding with sodium citrate, resulting in a significant upregulation of intracellular glutamine levels [16]. Glutamine, an essential intracellular metabolic fuel, can be rapidly re-catabolized into AKG to enter the TCA cycle when the cell experiences the energy requirement. Moreover, glutamine is involved in intracellular nitrogen-related anabolism and catabolism, which is an intracellular biosynthesis precursor of some amino acids and nucleotides [23–25].

Glutathione is synthesized from glutamate, cysteine, and glycine by a sequential reaction catalyzed by  $\gamma$ -glutamylcysteine synthetase ( $\gamma$ -GCS) and glutathione synthase [26]. The previous report has demonstrated that the optimum pH for glutathione production by *P. pastoris* was 3.5, and weak acid stress can effectively increase the enzymatic activity of  $\gamma$ -GCS [27]. The intracellular glutathione levels saw a significant downregulation since the sodium citrate supplement could increase the pH, reaching about 6.0 in the fermentation broth. Briefly, the feeding of sodium citrate will affect the enzymatic activity of  $\gamma$ -GCS, resulting in a significant downregulation of intracellular glutathione content.

In addition, glutathione, a catabolic product of SAM, generates cysteine and consumes large amounts of ATP and glutamate, which is the synthetic precursor of AKG, SAM, and the primary energy source for cellular metabolism. Therefore, the decrease of glutathione levels indicated that the feeding of sodium citrate effectively reduced the metabolism associated with the SAM consumption pathway. Meanwhile, the supplementation would contribute to the accumulation of AKG. On the one hand, the increase in TCA cycle flux could promote the synthesis of ATP, and on the other hand, it would also prevent the additional consumption of ATP involved in the synthesis of glutathione. Therefore, adequate energy precursors could be provided for the biosynthesis of SAM. In addition, glutathione could alleviate intracellular oxidative stress by oxidizing to oxidized glutathione. In this study, the downregulation would allow an increased level of intracellular active oxygen, leading to oxidative stress injury [28]. Therefore, the consequences could bring a decreased growth rate in terms of feeding with sodium citrate.

Carnitine can promote the oxidative degradation of fatty acids to provide energy [29]. The energy demand for cellular metabolism could be supplied through the oxidation of fatty acids under ATP limitation. Thus, there may be a high demand for carnitine levels. In this study, the carnitine content showed a significant down-regulation, possibly due to the fact that feeding sodium citrate could alleviate the intracellular energy metabolism. In addition, the precursors of carnitine synthesis are L-methionine and lysine, and the down-regulation of carnitine indicated that the amount of intracellular L-methionine and lysine used for carnitine synthesis was reduced. Meanwhile, the down-regulation could save the consumption of aspartic acid and the non-product anabolic metabolism of L-methionine. Therefore, the trend could enhance the utilization of L-methionine for the synthesis product SAM.

Overall, the results suggested that the addition of sodium citrate significantly affected the intracellular levels of some amino acid-like metabolites. Specifically, the addition of sodium citrate might effectively reduce the catabolic pathway of SAM and lessen the non-product synthesis of the precursor L-methionine. In addition, the changes in metabolite levels contributed to an increase in the metabolic flux of the intracellular TCA cycle, effectively increasing the intracellular activity of oxidative phosphorylation.

### 3.3.3. Clustering Analysis of Differential Metabolites Related to Organic Acid Metabolism

Organic acids are a class of acidic organic compounds containing carboxyl groups that are widely present in living organisms. They play a critical role in various intracellular biochemical pathways, including energy metabolism, formation of amino acid biosynthetic precursors, and regulation of environmental adaptation [30]. The pathways related to organic acid metabolism include the TCA cycle, glyoxylate and dicarboxylic acid metabolic pathway, and 2-oxocarboxylic acid metabolism, which involve significantly different metabolites as shown in Figure 3c. The citric acid, cis-aconitate, cumulinic acid, and 2-oxoadipic acid were up-regulated considerably compared with the control group. In contrast, 5-aminosalicylic acid and 4-oxobutyric acid were significantly down-regulated in the experimental group.

The feeding of sodium citrate can effectively increase the intracellular citric acid content and further increase the level of cis-aconitate through the TCA cycle, which will help to increase the metabolic flux of the TCA cycle. Moreover, the increased energy cofactors NADH and FADH<sub>2</sub> could provide sufficient free energy for ATP synthesis through the electron transport chain. In addition, 2-oxoadipic acid is a metabolite of the lysine catabolic pathway [31]. Lysine metabolism produces 2-oxoadipic acid, which is metabolized to acetyl coenzyme A via dehydrodecarboxylation and  $\beta$ -oxidation in the lysine metabolic pathway to enter the TCA cycle. Briefly, the upregulation of the intracellular level of 2-oxoadipic acid will help to increase the intracellular acetyl coenzyme A content and further increase the level of oxidative phosphorylation.

The results showed that the addition of sodium citrate promoted the upregulation of intracellular levels of some organic acid metabolites, which contributed to the increase of metabolic fluxes and intracellular levels of oxidative phosphorylation in the TCA cycle. On the one hand, it could effectively alleviate the deficiency of intracellular energy metabolism caused by excessive L-methionine supplementation. On the other hand, the increase of oxidative phosphorylation levels might generate the damage of oxidative stress caused by excessive intracellular active oxygen, which affects the cell growth and metabolism. Therefore, optimization of the above situation needs to be subsequently improved.

### 3.4. Metabolic Flux Analysis

Metabolic flux analysis was performed for the fermentation process in the experimental and control groups during the metabolomics analysis. The period for the metabolic flux analysis was 12 h after sodium citrate supplementation (induction phase 24–36 h). The results of the carbon balance analysis are shown in Table 1.

**Table 1.** The metabolic parameters of control and experimental groups in the induction phase 24–36h.

Metabolic Parameters	Control Group	Experimental Group
$q_{\text{MeOH}}$ (mmol/gDCW/h)	$9.25 \pm 0.09$	$11.24 \pm 0.15$
$q_{\text{SAM}}$ (mmol/gDCW/h)	$0.0015 \pm 0.0002$	$0.0032 \pm 0.0003$
$q_{\text{Tri.Ci}}$ (mmol/gDCW/h)	0	0.160
$q_{\text{L-Met}}$ (mmol/gDCW/h)	$0.041 \pm 0.0029$	$0.035 \pm 0.0021$
$q_{\text{CO}_2}$ (mmol/gDCW/h)	$9.29 \pm 0.31$	$12.04 \pm 0.28$
$q_{\text{O}_2}$ (mmol/gDCW/h)	$19.49 \pm 0.15$	$25.62 \pm 0.36$
Carbon recoveries <sup>1</sup> (%)	$98.58 \pm 0.08$	$97.70 \pm 0.10$

$$^1 \text{ Carbon recoveries} = [(q_{\text{SAM}} * 15 + q_{\text{CO}_2} * 1) / (q_{\text{MeOH}} * 1 + q_{\text{Tri.Ci}} * 6 + q_{\text{L-Met}} * 5)] \times 100\%.$$

Fermentation parameters and intracellular metabolic fluxes changed considerably in the batch with sodium citrate supplementation. Specifically, the  $q_{\text{CO}_2}$  and  $q_{\text{O}_2}$  of the experimental group increased by 29.60% and 31.45%, respectively, compared with the control group, indicating that the addition of sodium citrate had a promotion effect on the respiratory metabolism. In addition, the  $q_{\text{MeOH}}$  in the experimental group increased by 21.51% and  $q_{\text{L-Met}}$  decreased by 14.63%, compared with the control group, and the specific production rate of SAM increased by 113.33%. The results indicated that the addition of sodium citrate could facilitate the metabolization of the substrate and promote the growth to maintain high-density fermentation, while also generating and accumulating some precursors required for SAM synthesis through central carbon metabolism.

The metabolic flux distribution of the central carbon metabolism pathway at 24–36 h during the methanol induction stage is shown in Figure 4. It was found that the fluxes of intracellular metabolic pathways changed significantly after the supplementation of sodium citrate. Specifically, the reaction fluxes for the pentose phosphate (PP) pathway saw a 22.08% increase in the experimental group compared with the control group. The reaction flux increased by 20.45% for the glycolysis pathway. In addition, the reaction fluxes of the TCA cycle and the glyoxylate cycle pathway witnessed 24.19% and 29.32% enhancement. The results demonstrated that the feeding of sodium citrate considerably changed the flux distribution of central carbon metabolism. Briefly, the fluxes flowed more to the TCA cycle and the glyoxylate cycle, which effectively alleviated the deficiency of intracellular energy metabolism and provided sufficient precursors for SAM production.

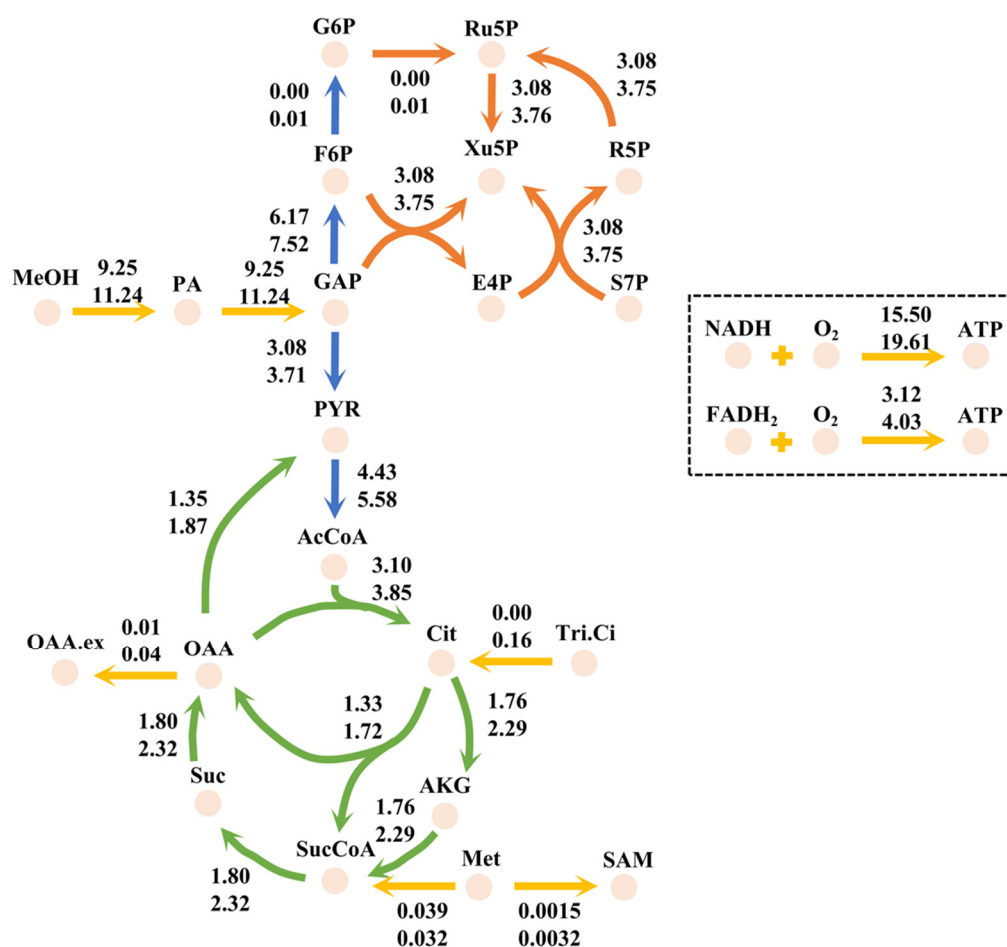


**Figure 4.** Metabolic flux analysis between control and experimental groups during the induction phase 24–36 h (The numbers near the reaction represent metabolic flux values, mmol/gDCW/h. The upper values are for the control group and the lower values are for the experimental group.). Abbreviations: G6P, glucose-6-phosphate; F6P, fructose 6-phosphate; R5P, ribose-5-phosphate; Ru5P, ribulose 5-phosphate; Xu5P, xylulose 5-phosphate; GAP, glyceraldehyde-3-phosphate; PYR, pyruvic acid; AcCoA, acetyl coenzyme A; Cit, citrate; AKG, 2-oxoglutarate; SucCoA, succinyl coenzyme A; Suc, succinic; OAA, oxaloacetate; Met, L-methionine; Tri.Ci, sodium citrate; MeOH, Methanol; PA, formaldehyde; OAA.ex, extracellular oxaloacetate.

### 3.5. Analysis of Metabolic Regulatory Mechanisms

The possible regulatory mechanism of sodium citrate on the cellular metabolism is shown in Figure 5. For the methanol metabolism pathway, the flux distribution results showed an increase of 21.51% in its reaction flux. It is speculated that it may be related to the increased activity of alcohol oxidase AOX1 after sodium citrate supplementation. DHA, converted from methanol to glyceraldehyde 3-phosphate (GAP), observed a significant upregulation according to the results mentioned above in metabolomics, which could serve as corroboration for the increased activity of alcohol oxidase AOX1. A previous report [32] has shown that a higher alcohol oxidase activity can be detected in *P. pastoris* grown in a medium with DHA as the sole carbon source. In addition, the results suggested that DHA can induce the initiation of PAOX1 and that the upregulation of DHA levels can contribute to the activity of alcohol oxidase AOX1.

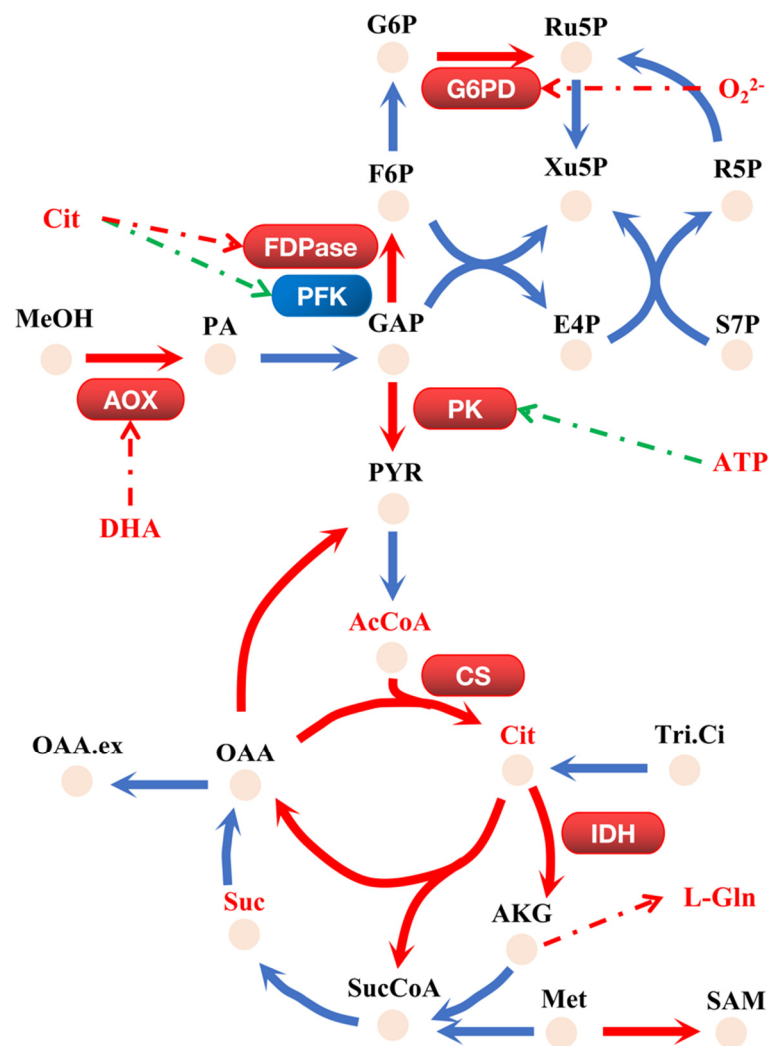


**Figure 5.** Putative regulatory mechanisms revealed by integrated untargeted metabolomics and metabolic flux analysis regarding the effect of sodium citrate on the fermentation of *P. pastoris* (The red capsules and red arrows indicate the enzymes whose activity appears to be increased and the corresponding reactions; the red font indicates the metabolites whose intracellular content appears to be up-regulated; the red and green dashed lines indicate the activating and inhibiting effects, respectively; and the blue capsules indicate the enzymes whose activity is inhibited. AOX is alcohol oxidase, G6PD is glucose-6-phosphate dehydrogenase, PFK is phosphofructokinase, FDPase is fructose 1,6-diphosphate phosphatase, PK is pyruvate kinase, CS is citrate synthase, IDH is isocitrate dehydrogenase).

The flux distribution witnessed a 20.45% increase for the EMP pathway according to the metabolic flux analysis. In this study, there was no conventional substrate glucose intake. The alteration of the EMP pathway was mainly caused by the flux change of the methanol metabolic pathway after the supplementation of sodium citrate. Both the GAP generated from the methanol metabolic pathway and the replenishment pathway from oxaloacetate (OAA) would provide precursors for Pyr generation, and sufficient precursors would effectively increase the flux of the EMP pathway. Metabolomic data revealed that metabolites such as alanine, phenylalanine, and cyclic adenosine monophosphate (cAMP), which can have an inhibitory effect on pyruvate kinase (PK) activity, all presented the down-regulation trend. Therefore, it was hypothesized that the changes in intracellular metabolites after sodium citrate supplementation led to an increase in PK activity, increasing metabolic fluxes of the EMP pathway. A previous report [33] has demonstrated

that PK was inhibited by high concentrations of ATP. However, the flux of the reaction catalyzed was up-regulated in this study. The results indicated that although the addition of sodium citrate could act as an alleviator of intracellular energy metabolism and relieve the metabolic burden caused by product synthesis, it did not allow the intracellular ATP level to be at a high level, which does not cause an inhibitory effect on PK. In addition, the intracellular citric acid content appeared significantly up-regulated after sodium citrate supplementation. According to the KEGG Enzyme Database (<https://www.kegg.org>, accessed on 4 December 2019), the activity of fructose-1,6-bisphosphatase (FDPase), a key enzyme in the gluconeogenesis pathway that catalyzes the production of F6P from GAP, is activated by the citric acid. In contrast, the activity of fructose phosphokinase (PFK), which catalyzes the production of GAP from F6P, is inhibited by citric acid. Therefore, the results could cause a significant increase in the reaction flux of the gluconeogenesis pathway and provide the PP pathway with more precursors.

The PP pathway is a multifunctional metabolic pathway that generates NADPH to provide reducing power in response to oxidative stress, as well as ribose 5-phosphate for nucleotide coenzymes and nucleotide biosynthesis [34]. Glucose-6-phosphate dehydrogenase (G6PD) is the first and rate-limiting enzyme of the pathway, and its activity will determine the metabolic flux variation of the entire PP pathway. In this study, a 22.08% enhancement for the PP pathway in flux distribution was observed. A previous study has illustrated that the catalytic capacity of G6PD was significantly activated under oxidative stress [35]. In this study, the supplementation of sodium citrate promoted an increase in the level of oxidative phosphorylation, which in turn caused oxidative stress. The latter could activate the catalytic capacity of G6PD. Therefore, the increased fluxes of the PP pathway could provide the cell with energy cofactors and precursors for the biosynthesis of nucleotide coenzymes such as NAD<sup>+</sup>, NADP<sup>+</sup>, and FAD. In addition, it can supply the required Xu5P for methanol metabolism, which effectively promotes methanol utilization.

Additionally, the flux distributions of the TCA cycle and glyoxylate cycle saw 24.19% and 29.32% enhancement according to the metabolic flux analysis. The intracellular citric acid and cis-aconitic acid contents were significantly up-regulated by the addition of sodium citrate, and sufficient precursors could effectively increase the flux of the TCA cycle. It has been proven that sodium citrate supplementation in yeast cells significantly increased the mRNA transcript levels and enzyme activity of isocitrate dehydrogenase (IDH) in the TCA cycle [36]. AKG, a product of the IDH-catalyzed reaction, showed a significant upregulation of its metabolite L-glutamine (L-Gln) as well as succinate (Suc) according to metabolomic data, which could serve as corroboration for the increased IDH activity. In addition, a previous report has shown that acetyl coenzyme A (AcCoA) can allosterically activate the biological activity of citrate synthase (CS) [37]. Metabolomic data revealed that the intracellular levels of succinyl coenzyme A (SucCoA), a citrate inhibitor, did not change significantly after sodium citrate supplementation. Meanwhile, the content of AcCoA showed a more significant upregulation, which could effectively activate the CIT activity and allow more flux from the EMP pathway into the TCA cycle. Similarly, the upregulation of CIT activity could also promote the metabolic flux of the glyoxylate cycle.

#### 4. Conclusions

The effects of sodium citrate addition on the intracellular metabolism of *P. pastoris* were investigated by liquid chromatography-mass spectrometry-based untargeted metabolomics and metabolic flux analysis. The results showed that 1247 metabolites were identified, and 41 significantly different metabolites and 13 significant metabolic pathways associated with them were screened. The feeding of sodium citrate had a more substantial effect on the intracellular metabolic levels of organic acids and amino acid metabolites. The changes in these compounds provided sufficient precursors for SAM biosynthesis. Meanwhile, SAM catabolic pathways appeared to be weakened, which would contribute to SAM intracellular accumulation. In addition, metabolic flux analysis was carried out for 24–36 h in the methanol induction phase between the control and experimental groups. The

results showed that the reaction fluxes of most intracellular metabolic pathways were increased after the addition of sodium citrate, which laid the foundation for the supply of precursors for the product SAM biosynthesis. Finally, the possible mechanism of the effect of sodium citrate addition on cellular metabolism was explored by integrating metabolomics and fluxomics. Therefore, this study can improve and deepen the understanding of the mechanism of the effect of sodium citrate on the intracellular metabolism of *P. pastoris* strains, which is of great significance to accelerate the process of large-scale application of SAM.

**Supplementary Materials:** The following supporting information can be downloaded at: <https://www.mdpi.com/article/10.3390/fermentation8120681/s1>, Figure S1. Physiological profiles of *P. pastoris* at the rate of 0.2 g/L/h and 0.4 g/L/h L-methionine supplementation in fed-batch cultivations; Figure S2. Physiological profiles of *P. pastoris* fermentation under supplementation with sodium citrate; Figure S3. The multivariate statistical analysis for the samples. Volcano plot of (a) positive ion mode and (b) negative ion mode (color correlates with differential metabolite up- and down-regulation, marked with qualitative names, up- and down-regulation multiplicity); OPLS-DA score in (c) positive ion mode and (d) negative ion mode; Permutation test of OPLS-DA model in (e) positive ion mode and (f) negative ion mode; Figure S4. The PCA score. (a) Positive ion mode; (b) Negative ion mode; Table S1: The simplified metabolic network model of *P. pastoris*.; Table S2. The significantly upregulated differential metabolites; Table S3. The significantly downregulated differential metabolites.

**Author Contributions:** Conceptualization, M.H. and J.Q.; methodology, F.X. and W.X.; software, W.S. and L.D.; validation, W.X., W.S. and L.D.; formal analysis, F.X. and W.X.; investigation, W.X.; data curation, F.X. and W.X.; writing—original draft preparation, F.X. and W.X.; writing—review and editing, M.H.; visualization, F.X. and W.X.; supervision, M.H.; project administration, M.H.; funding acquisition, M.H. All authors have read and agreed to the published version of the manuscript.

**Funding:** This work was financially supported by a grant from National Natural Science Foundation of China (Grant No. 32071461), National Key Research and Development Program of China (Grant No. 2019YFA0904300).

**Institutional Review Board Statement:** Not applicable.

**Informed Consent Statement:** Not applicable.

**Data Availability Statement:** The data presented in this study are available on request from the corresponding author because of its usage in the ongoing study.

**Conflicts of Interest:** The authors declare no conflict of interest.

## References

1. Mischoulon, D.; Alpert, J.E.; Arning, E.; Bottiglieri, T.; Fava, M.; Papakostas, G.I. Bioavailability of S-adenosyl methionine and impact on response in a randomized, double-blind, placebo-controlled trial in major depressive disorder. *J. Clin. Psychiat.* **2012**, *73*, 843–848. [[CrossRef](#)] [[PubMed](#)]
2. Chen, Y.W.; Lou, S.Y.; Fan, L.H.; Zhang, X.; Tan, T.W. Control of ATP concentration in *Escherichia coli* using synthetic small regulatory RNAs for enhanced S-adenosylmethionine production. *FEMS Microbiol. Lett.* **2015**, *362*, 1–8. [[CrossRef](#)] [[PubMed](#)]
3. Chen, H.L.; Wang, Z.L.; Cai, H.B.; Zhou, C.L. Progress in the microbial production of S-adenosyl-L-methionine. *World J. Microbiol. Biotechnol.* **2016**, *32*, 153. [[CrossRef](#)] [[PubMed](#)]
4. Huang, Y.; Gou, X.; Hu, H.; Xu, Q.; Lu, Y.; Cheng, J. Enhanced S-adenosyl-L-methionine production in *Saccharomyces cerevisiae* by spaceflight culture, overexpressing methionine adenosyltransferase and optimizing cultivation. *J. Appl. Microbiol.* **2012**, *112*, 683–694. [[CrossRef](#)] [[PubMed](#)]
5. Parashar, S.; Cheishvili, D.; Arakelian, A.; Hussain, Z.; Tanvir, I.; Khan, H.A.; Szyf, M.; Rabbani, S.A. S-adenosylmethionine blocks osteosarcoma cells proliferation and invasion in vitro and tumor metastasis in vivo: Therapeutic and diagnostic clinical applications. *Cancer Med.* **2015**, *4*, 732–744. [[CrossRef](#)] [[PubMed](#)]
6. Chu, J.; Qian, J.C.; Zhuang, Y.P.; Zhang, S.L.; Li, Y.R. Progress in the research of S-adenosyl-L-methionine production. *Appl. Microbiol. Biotechnol.* **2013**, *97*, 41–49. [[CrossRef](#)] [[PubMed](#)]
7. Macauley-patrick, S.; Fazenda, M.L.; Mcneil, B.; Harvey, L.M. Heterologous protein production using the *Pichia pastoris* expression system. *Yeast* **2005**, *22*, 249–270. [[CrossRef](#)]

8. Hayakawa, K.; Matsuda, F.; Shimizu, H. Metabolome analysis of *Saccharomyces cerevisiae* and optimization of culture medium for S-adenosyl-L-methionine production. *AMB Express*. **2016**, *6*, 38. [[CrossRef](#)]
9. Wang, Y.L.; Wang, D.H.; Wei, G.Y.; Wang, C.F. Improved co-production of S-adenosylmethionine and glutathione using citrate as an auxiliary energy substrate. *Bioresour. Technol.* **2013**, *131*, 28–32. [[CrossRef](#)]
10. Qin, X.L.; Lu, J.J.; Zhang, Y.; Wu, X.L.; Qiao, X.F.; Wang, Z.P.; Chu, J.; Qian, J.C. Engineering *Pichia pastoris* to improve S-adenosyl-L-methionine production using systems metabolic strategies. *Biotechnol. Bioeng.* **2020**, *117*, 1436–1445. [[CrossRef](#)] [[PubMed](#)]
11. Hu, X.Q.; Chu, J.; Zhang, S.L.; Zhuang, Y.P.; Wang, Y.H.; Zhu, S.; Zhu, Z.G.; Yuan, Z. A novel feeding strategy during the production phase for enhancing the enzymatic synthesis of S-adenosyl-L-methionine by methylotrophic *Pichia pastoris*. *Enzyme Microb. Technol.* **2007**, *40*, 669–674. [[CrossRef](#)]
12. Hu, H.; Qian, J.C.; Chu, J.; Wang, Y.H.; Zhuang, Y.P.; Zhang, S.L. Optimization of L-methionine feeding strategy for improving S-adenosyl-L-methionine production by methionine adenosyltransferase overexpressed *Pichia pastoris*. *Appl. Microbiol. Biot.* **2009**, *83*, 1105–1114. [[CrossRef](#)] [[PubMed](#)]
13. Xu, F.; Ke, X.; Hong, M.; Huang, M.Z.; Chen, C.C.; Tian, X.W.; Hang, H.F.; Chu, J. Exploring the metabolic fate of propanol in industrial erythromycin-producing strain via <sup>13</sup>C labeling experiments and enhancement of erythromycin production by rational metabolic engineering of *Saccharopolyspora erythraea*. *Biochem. Biophys. Res. Commun.* **2021**, *542*, 73–79. [[CrossRef](#)] [[PubMed](#)]
14. Lu, H.Z.; Liu, X.Y.; Huang, M.Z.; Xia, J.Y.; Chu, J.; Zhuang, Y.P.; Zhang, S.L.; Noorman, H. Integrated isotope-assisted metabolomics and <sup>13</sup>C metabolic flux analysis reveals metabolic flux redistribution for high glucoamylase production by *Aspergillus niger*. *Microb. Cell Fact.* **2015**, *14*, 147. [[CrossRef](#)]
15. Abdelrazig, S.; Ortori, C.A.; Doherty, M.; Valdes, A.M.; Chapman, V.; Barrett, D.A. Metabolic signatures of osteoarthritis in urine using liquid chromatography-high resolution tandem mass spectrometry. *Metabolomics* **2021**, *17*, 29. [[CrossRef](#)] [[PubMed](#)]
16. Liu, P.; Huang, M.Z.; Guo, M.L.; Qian, J.C.; Lin, W.L.; Chu, J.; Zhuang, Y.P.; Zhang, S.L. Combined <sup>13</sup>C-assisted metabolomics and metabolic flux analysis reveals the impacts of glutamate on the central metabolism of high  $\beta$ -galactosidase-producing *Pichia pastoris*. *Bioresour. Bioprocess.* **2016**, *3*, 47. [[CrossRef](#)] [[PubMed](#)]
17. Nie, Y.S.; Huang, M.Z.; Lu, J.J.; Qian, J.C.; Lin, W.L.; Chu, J.; Zhuang, Y.P.; Zhang, S.L. Impacts of high  $\beta$ -galactosidase expression on central metabolism of recombinant *Pichia pastoris* GS115 using glucose as sole carbon source via (<sup>13</sup>)C metabolic flux analysis. *J. Biotechnol.* **2014**, *187*, 124–134. [[CrossRef](#)]
18. Jordà, J.; Suarez, C.; Carnicer, M.; ten Pierick, A.; Heijnen, J.J.; van Gulik, W.; Ferrer, P.; Albiol, J.; Wahl, A. Glucose-methanol co-utilization in *Pichia pastoris* studied by metabolomics and instationary <sup>13</sup>C flux analysis. *BMC Syst. Biol.* **2013**, *7*, 17. [[CrossRef](#)]
19. Heyland, J.; Fu, J.N.; Blank, L.M.; Schmid, A. Quantitative physiology of *Pichia pastoris* during glucose-limited high-cell density fed-batch cultivation for recombinant protein production. *Biotechnol. Bioeng.* **2010**, *107*, 357–368. [[CrossRef](#)] [[PubMed](#)]
20. Heyland, J.; Fu, J.N.; Blank, L.M.; Schmid, A. Carbon metabolism limits recombinant protein production in *Pichia pastoris*. *Biotechnol. Bioeng.* **2011**, *108*, 1942–1953. [[CrossRef](#)]
21. Xu, F.; Lu, J.; Ke, X.; Shao, M.H.; Huang, M.Z.; Chu, J. Reconstruction of the Genome-Scale Metabolic Model of *Saccharopolyspora erythraea* and Its Application in the Overproduction of Erythromycin. *Metabolites* **2022**, *12*, 509. [[CrossRef](#)] [[PubMed](#)]
22. Ye, R.; Huang, M.Z.; Lu, H.Z.; Qian, J.C.; Lin, W.L.; Chu, J.; Zhuang, Y.P.; Zhang, S.L. Comprehensive reconstruction and evaluation of *Pichia pastoris* genome-scale metabolic model that accounts for 1243 ORFs. *Bioresour. Bioprocess.* **2017**, *4*, 22. [[CrossRef](#)] [[PubMed](#)]
23. Soberon, M.; Olamendi, J.; Rodriguez, L.; González, A. Role of glutamine aminotransferase in glutamine catabolism by *Saccharomyces cerevisiae* under microaerophilic conditions. *J. Gen. Microbiol.* **1989**, *135*, 2693–2697. [[CrossRef](#)] [[PubMed](#)]
24. Fayyad-Kazan, M.; Feller, A.; Bodo, E.; Boeckstaens, M.; Marini, A.M.; Dubois, E.; Georis, I. Yeast nitrogen catabolite repression is sustained by signals distinct from glutamine and glutamate reservoirs. *Mol. Microbiol.* **2016**, *99*, 360–379. [[CrossRef](#)]
25. Ding, M.Z.; Wang, X.; Yang, Y.; Yuan, Y.J. Metabolomic study of interactive effects of phenol, furfural, and acetic acid on *Saccharomyces cerevisiae*. *OMICS* **2011**, *15*, 647–653. [[CrossRef](#)]
26. Lu, S.C. Glutathione synthesis. *Biochim. Biophys. Acta* **2013**, *1830*, 3143–3153. [[CrossRef](#)]
27. He, J.Y.; Deng, J.J.; Zheng, Y.H.; Gu, J. A synergistic effect on the production of S-adenosyl-L-methionine in *Pichia pastoris* by knocking in of S-adenosyl-L-methionine synthase and knocking out of cystathionine-beta synthase. *J. Biotechnol.* **2006**, *126*, 519–527. [[CrossRef](#)]
28. Sulheim, S.; Kumelj, T.; van Dissel, D.; Salehzadeh-Yazdi, A.; Du, C.; van Wezel, G.P.; Nieselt, K.; Almaas, E.; Wentzel, A.; Kerkhoven, E.J. Enzyme-Constrained Models and Omics Analysis of *Streptomyces coelicolor* Reveal Metabolic Changes that Enhance Heterologous Production. *iScience* **2020**, *23*, 101525. [[CrossRef](#)]
29. Pekala, J.; Patkowska-Sokoła, B.; Bodkowski, R.; Jamroz, D.; Nowakowski, P.; Lochyński, S.; Librowski, T. L-carnitine-metabolic functions and meaning in humans life. *Curr. Drug Metab.* **2011**, *12*, 667–678. [[CrossRef](#)]
30. Pook, C.; Diep, T.T.; Yoo, M.J.Y. Simultaneous Quantification of Organic Acids in Tamarillo (*Solanum betaceum*) and Untargeted Chemotyping Using Methyl Chloroformate Derivatization and GC-MS. *Molecules* **2022**, *27*, 1314. [[CrossRef](#)]
31. Shibata, K.; Yasui, M.; Sano, M.; Fukuwatari, T. Fluorometric determination of 2-oxoadipic acid, a common metabolite of tryptophan and lysine, by high-performance liquid chromatography with pre-chemical derivatization. *Biosci. Biotechnol. Biochem.* **2011**, *75*, 185–187. [[CrossRef](#)]

32. Koning, W.; Gleeson, M.A.G.; Harder, W.; Dijkhuizen, L. Regulation of methanol metabolism in the yeast *Hansenula polymorpha*. *Arch. Microbiol.* **1987**, *147*, 375–382. [[CrossRef](#)]
33. Gosalvez, M.; Pérez-García, J.; Weinhouse, S. Competition for ADP between pyruvate kinase and mitochondrial oxidative phosphorylation as a control mechanism in glycolysis. *Eur. J. Biochem.* **1974**, *46*, 133–140. [[CrossRef](#)] [[PubMed](#)]
34. Masi, A.; Mach, R.L.; Mach-Aigner, A.R. The pentose phosphate pathway in industrially relevant fungi: Crucial insights for bioprocessing. *Appl. Microbiol. Biotechnol.* **2021**, *105*, 4017–4031. [[CrossRef](#)] [[PubMed](#)]
35. Wang, Y.P.; Zhou, L.S.; Zhao, Y.Z.; Wang, S.W.; Chen, L.L.; Liu, L.X.; Ling, Z.Q.; Hu, F.J.; Sun, Y.P.; Zhang, J.Y.; et al. Regulation of G6PD acetylation by SIRT2 and KAT9 modulates NADPH homeostasis and cell survival during oxidative stress. *EMBO J.* **2014**, *33*, 1304–1320. [[CrossRef](#)] [[PubMed](#)]
36. Chen, H.L.; Wang, Z.; Wang, Z.L.; Dou, J.; Zhou, C.L. Improving methionine and ATP availability by MET6 and SAM2 co-expression combined with sodium citrate feeding enhanced SAM accumulation in *Saccharomyces cerevisiae*. *World J. Microbiol. Biotechnol.* **2016**, *32*, 56. [[CrossRef](#)]
37. Anderson, D.H.; Duckworth, H.W. In vitro mutagenesis of *Escherichia coli* citrate synthase to clarify the locations of ligand binding sites. *J. Biol. Chem.* **1988**, *263*, 2163–2169. [[CrossRef](#)]